Magnetic Resonance Imaging 62 (2019) 10–17

Contents lists available at ScienceDirect

Magnetic Resonance Imaging

journal homepage: www.elsevier.com/locate/mri

Original contribution

Differentiation between sinonasal natural killer/T-cell lymphomas and diffuse large B-cell lymphomas by RESOLVE DWI combined with conventional MRI

Mengge He[a,b,c,1], Zuohua Tang[c,*,1], Jinwei Qiang[b,**], Zebin Xiao[c], Zhongshuai Zhang[d]

[a] The Shanghai Institution of Medical Imaging, Zhongshan Hospital, Fudan University, Shanghai 200032, China
[b] Department of Radiology, Jinshan Hospital, Fudan University, Shanghai 201508, China
[c] Department of Radiology, Eye and ENT Hospital, Fudan University, Shanghai 200031, China
[d] Scientific Marketing, Diagnostic Imaging, Siemens Healthcare, Shanghai 201318, China

ARTICLE INFO

Keywords:
Sinonasal neoplasm
Natural killer/T-cell lymphoma
Diffuse large B-cell lymphoma
Diffusion-weighted imaging
Magnetic resonance imaging

ABSTRACT

Objective: To explore the feasibility of using RESOLVE DWI combined with conventional magnetic resonance imaging (MRI) to discriminate between sinonasal NKTLs and DLBCLs and to investigate the correlation between ADC value and Ki-67 expression in **the two** subtypes of NHLs.

Materials and methods: Sixty patients with NKTLs and twenty-six patients with DLBCLs in the sinonasal region who were confirmed by histopathology underwent high-resolution DWI and conventional MRI. The apparent diffusion coefficients (ADCs) and conventional MRI features associated with NKTLs and DLBCLs were compared using multivariate logistic regression. Receiver operating characteristic (ROC) curve analysis was performed, and the area under the curve (AUC) values for conventional MRI and MRI in combination with DWI were compared to determine the diagnostic performances of the approaches in the differentiation of NKTLs and DLBCLs. Spearman's rank correlations were used to analyze the correlation between ADC value with the higher AUC and Ki-67 expression.

Results: For conventional MRI, localization in the nasal cavity and poor or moderate enhancement indicated an NKTL, whereas localization in the paranasal sinus and intense enhancement indicated a DLBCL, with sensitivity, specificity and area under the curve(AUC)value of 88.5%, 85.0% and 0.883, respectively. A combination with a cut-off ADC value of 0.646×10^{-3} mm^2/s yielded sensitivity, specificity and AUC values of 100.0%, 80.0% and 0.951, respectively. A significant difference between the AUCs for conventional MRI and MRI in combination with DWI ($p = 0.02$) was identified. Ki-67 expression of NKTLs was significantly lower than that of DLBCLs ($p < 0.001$). Besides, there was an inversely poor correlation between them in the overall sample ($r = -0.395$, $p < 0.001$). However, the ADC value was not significantly correlated with Ki-67 LI in neither NKTLs nor DLBCLs (both $p > 0.05$).

Conclusions: Location and enhancement degree were the most valuable conventional MRI features for differentiating between NKTLs and DLBCLs. A combination of DWI and MRI could significantly improve the differential performance. ADC values may be used to noninvasively evaluate the proliferation level of sinonasal NHLs.

1. Introduction

As the second most common malignancy in the sinonasal region (only squamous cell neoplasms are more common), non-Hodgkin's lymphomas (NHLs) account for approximately 14% of all malignancies [1]. Among NHLs, diffuse large B-cell lymphomas (DLBCLs) are reported to be the most common type (30%–40%) in the western population, whereas natural killer/T-cell lymphomas (NKTLs) only account for 1% of NHLs in Caucasian cases; however, NKTLs are the most common type (7%–10%) in East Asia and Latin America [2–4]. The two

* Correspondence to: Z. Tang, Department of Radiology, Eye & ENT Hospital of Shanghai Medical School, Fudan University, 83 Fenyang Road, Shanghai 200031, PR China.
** Correspondence to: J. Qiang, Department of Radiology, Jinshan Hospital of Shanghai Medical School, Fudan University, 1508 Longhang Road, Shanghai 201508, PR China.
E-mail addresses: tzh518sunny@163.com (Z. Tang), dr.jinweiqiang@163.com (J. Qiang).
[1] The first two authors contributed equally to this study.

https://doi.org/10.1016/j.mri.2019.06.011
Received 18 January 2019; Received in revised form 12 June 2019; Accepted 14 June 2019

types of lymphomas have distinct treatments and prognoses [5,6]. A combination of chemotherapy and radiotherapy for early-stage disease and chemotherapy alone (L-asparaginase-based therapy, such as the SMILE regimen) for late-stage disease have been shown to improve the outcome of NKTL patients [7]; furthermore, the addition of rituximab to the CHOP regimen has significantly improved the overall survival rate for elderly DLBCL patients [8]. The disease-specific survival rate of sinonasal NKTLs is significantly lower than that of sinonasal DLBCLs [5]. Therefore, early and precise diagnosis and treatment of NHLs have important clinical implications.

However, endoscopic excisional biopsy, the gold standard for a definitive diagnosis, faces challenges. Unlike carcinomas that arise in a dysplastic epithelium, lymphomas are of subepithelial origin. They may be masked by an overlying inflammatory, pleomorphic infiltration or by large areas of necrosis [9]. Thus, a superficial sampling may be negative for a deeper underlying malignant lymphoma [10]. Furthermore, the molecular diagnostic approaches demanded by complex cases, such as immunohistochemical staining and genetic techniques, often cause a substantial increase in diagnosis-related time, costs and patient anxiety [11]. Compared to invasive procedures, which are unable to determine the extent of the lesions, noninvasive imaging techniques, such as computed tomography (CT) and magnetic resonance imaging (MRI), offer advantages for early detection, staging and therapeutic decision-making in cases of sinonasal lymphoma [12]. However, the CT and MRI morphological features are nonspecific, and discrimination between the subtypes of NHLs remains a significant challenge.

Diffusion-weighted imaging (DWI) can offer better characterization of tissues and their physiological processes through the apparent diffusion coefficient (ADC) measurements [13], and it has been used to discriminate between benign and malignant head-and-neck masses, oropharyngeal lymphoma and squamous cell carcinoma and to characterize cervical lymph nodes [14]. A study by Wang et al. [1] showed that ADC values of NKTLs were significantly higher than those of DLBCLs. However, the sample size of the lymphoma cases was too small (n = 19) to evaluate the differential diagnostic ability of ADC values. Moreover, ADC value has the potential to reveal tumor microstructure like cellular density and proliferative activity in different neoplasms [15,16]. Studies have reported that ADC values are inversely correlated with proliferation potential (Ki-67) in lymphomas, indicating that ADC values can noninvasively evaluate the proliferation level and prognosis of lymphoma [17–19].

Recently, high-resolution DWI using readout-segmented echo-planar imaging (EPI), parallel imaging, and 2-dimensional navigator-based reacquisition (termed RESOLVE) has been shown to be significantly superior to the most widely used conventional single shot-EPI (SS-EPI) DWI in sinonasal lesions; the RESOLVE approach offers higher spatial resolution, which is crucial for discerning fine structures and for limiting susceptibility artifacts, which are inherent in sinonasal regions [20,21].

To the best of our knowledge, no studies have focused on the discrimination between NKTLs and DLBCLs. The present study aims to explore the feasibility of using RESOLVE DWI combined with conventional MRI to discriminate between sinonasal NKTLs and DLBCLs, and the correlation between ADC value and Ki-67 expression in **the two** subtypes of NHLs.

2. Materials and methods

2.1. Patients

This retrospective study was approved by our institutional review board, and the informed consent was waived. We reviewed our sinonasal lymphoma database. From January 2014 to February 2018, patients who satisfied the following criteria enrolled in the study: (a) patients with a sinonasal mass histologically confirmed to be NKTL or DLBCL; (b) patients with data from conventional MRI and RESOLVE DWI; (c) patients whose sinonasal mass had not undergone biopsy or treatment prior to MRI; and (d), patients who underwent MRI within 6 weeks before surgical resection or biopsy. Patients with recurrent tumors were excluded. Finally, a cohort of 86 patients (62 males, 24 females; average age 56.2 ± 15.5 years) consisting of 60 patients with NKTL (46 males and 14 females; mean age 54.9 ± 15.8 years) and 26 patients with DLBCL (16 males and 10 females; mean age 59.3 ± 14.7 years) was included in this study.

2.2. Conventional MRI protocol

All scans were performed on a 3.0 T MR scanner (MAGNETOM, Verio, Siemens, Erlangen, Germany) using a 12-channel head coil. Conventional MRI consisted of an axial fast spin-echo T1-weighted imaging (T1WI) (repetition time [TR]/echo time [TE] = 384/9.1 ms), an axial fast spin-echo T2-weighted imaging (T2WI) (TR/TE = 4000/99 ms) with or without fat suppression, and axial, coronal and sagittal contrast-enhanced T1WI with fat suppression before and after intravenous injection of 0.1 mmol/kg of Gd-DTPA (Magnevist, Bayer Schering, Berlin, Germany) at a rate of 2 ml/s, followed by 20 ml of 0.9% saline flush using a power injector, with a matrix of 640 × 592, a field of view (FOV) of 220 × 220 mm, and a thickness/gap of 6/0.6 mm.

2.3. Resolve DWI

For RESOLVE DWI, a readout-segmented EPI, parallel imaging and 2-dimensional navigator-based reacquisition were used; all DWI sequences were scanned axially. The parameters were as follows: TR/TE = 4700/66 ms; slice thickness/gap = 4/0.4 mm; slices = 25; bandwidth = 723 Hz/Px; matrix = 192 × 192; FOV = 240 × 240 mm; average = 1; readout segments = 7; echo spacing = 0.34 ms; voxel size = 1.6 × 1.3 × 4.0 mm; number of excitation = 1; gradient factors: b = 0, 1000 s/mm^2; diffusion directions = 3; and acquisition time = 2.55 min.

2.4. Imaging analysis

Two radiologists (readers 1 and 2), who had 5 and 8 years of experience in head and neck imaging, respectively, were blinded to the patients' histopathology before they independently analyzed the images. Disagreements were resolved through further discussion with a third radiologist (with 20 years of experience) to reach a consensus. The features of the masses, including location, laterality, size, signal intensity, inner component, margin, enhancement degree, bone destruction, and regional invasion were assessed. Based on the largest tumor slice, the locations were divided into (1) nasal cavity; (2) paranasal sinus; (3) nasal cavity and paranasal sinus (similar sizes in nasal cavity and paranasal sinus simultaneously), and the sizes of the tumors were measured. The signal intensities of the tumors on T1WI and T2WI were described as hypointense, isointense or hyperintense, by referring to adjacent muscles and mucosa, and as homogeneous or heterogeneous. The inner components included cystic/necrotic and hemorrhage. The margins of the tumors were described as well-defined (more than two-thirds of the border was sharply demarcated) or ill-defined (less than one-third of the border was sharply demarcated). The enhancement degree was described as poor (similar to muscles), moderate (greater than muscles) or intense (similar to the mucosa). Bone destruction was defined as the appearance of soft tissue signal replacing high bone marrow fat signal on T1WI, showing a similar enhancement degree as the tumor. Regional invasion was defined as a mucosa-based tumor that extended beyond the nasal cavity and paranasal sinus with 6 adjacent regions including: (1) nasal dorsum/adjacent cutaneous tissues; (2) nasopharyngeal/pterygoid region/oropharynx; (3) pterygopalatine fossa/infratemporal fossa; (4) orbital cavity/pterygoid musculature; (5)

palate/upper alveolar process; and (6) cervical lymph nodes (diameter > 1 cm).

To quantitatively analyze the data acquired from the RESOLVE DWI, 2 radiologists blinded to the clinical and histopathological data measured the ADC values of the tumors by drawing ROIs on ADC maps on a workstation (Syngo; Siemens Healthineers, Erlangen, Germany). Two ROI sampling methods were used: (1) polygonal ROI: the maximum tumor slice was selected and the ROI was manually drawn along the tumor margin. The measurement was repeated 3 times and averaged to obtain the representative ADC value, (2) small-round ROI: 3 small round ROIs (mean size 33.0 ± 14.0 mm^2) were placed inside the tumor on the same slice and 3 ADC values were averaged to obtain the representative value. All of the measurements were made carefully avoiding obvious cystic, necrotic or hemorrhagic areas. The measurements made by readers 1 and 2 were used to evaluate the interreader reproducibility and were averaged for statistical analysis.

2.5. Immunohistochemical analysis of Ki-67 expression

Ki-67 analyses were retrospectively performed by a pathologist (23 years of experience in sinonasal lymphoma pathology) who was blinded to the clinicopathological and MRI data. The Ki-67 labeling index (LI) was determined using the percentile of immunoreactive cells from 1000 malignant cells (×400), and scoring was decided in the areas with the highest number of positive nuclei (hot spot) inside the tumor using ImageJ software.

2.6. Statistical analysis

The demographic and MRI features between the NKTLs and DLBCLs were compared using the chi-square test or Fisher's exact test for categorical variables and the Mann–Whitney *U* test for noncategorical data. Receiver operating characteristic (ROC) curves were used to compare the diagnostic efficacy of the ADC values from the two types of ROI measurements. The ADC value with the higher area under the curve (AUC) value was enrolled into multivariate logistic regression analysis to explore the difference between NKTLs and DLBCLs. Odds ratios (ORs) were calculated using logistic regression models to determine the association between the histologic NHL types and the conventional MRI features as well as the ADC values. The diagnostic performance of conventional MRI versus a combination of MRI with RESOLVE DWI was evaluated. The statistical analyses were performed using MedCalc statistical software (version 15.2.2, Ostend, Belgium) and Statistical Package for the Social Sciences (Version 17.0, Chicago, IL). A p-value < 0.05 was considered to indicate a statistically significant difference.

Kappa analysis was used to assess the agreement between the two observers regarding the conventional MRI features of tumors. Kappa values < 0.40 were considered to indicate a poor agreement, values of 0.41 to 0.60 indicated a good agreement, and values of 0.61 to 1.00 indicated an excellent agreement [22]. The intraclass correlation coefficient (ICC) was used to evaluate the interreader reproducibility for the ADC measurements with 95% confidence intervals (CIs). An ICC > 0.75 was considered to indicate a good agreement [23].

Spearman's rank correlations were used to analyze the correlation between ADC value and Ki-67 LI. A correlation coefficient |r| < 0–0.5 was considered to be poor correlation, 0.5–0.8 was moderate correlation and |r| > 0.8 was defined as high correlation.

3. Results

As summarized in Table 1, the location (p < 0. 001), inner component (p = 0.025), enhancement degree (p = 0.012) and regional invasion of (3) pterygopalatine fossa/infratemporal fossa (p < 0.001) and (4) orbital cavity/pterygoid musculature (p < 0.001) were significantly different between NKTLs and DLBCLs. NKTLs exhibited significantly higher ADC values than did DLBCLs (p < 0.001) (Fig. 1). The differential performance of the ADC values from the polygonal ROIs were significantly higher than those generated using small round ROIs(p < 0.001) (Table 2, Fig. 2). Representative images are shown in Figs. 4 and 5.

Based on the results of the Mann–Whitney *U* test, chi-square test or Fisher's exact test, the locations, inner nature, enhancement degree, invaded regions of (3), (4), and ADC values from the polygonal ROIs were analyzed by logistic regression. As shown in Table 3, NKTLs were more likely to be seen in the nasal cavity (OR = 3.415 and 95% CI, 3.415–3.415), while DLBCLs were more often found in the paranasal sinus (OR = 621.771 and 95% CI, 621.771–621.771) or simultaneously

Table 1
The demographic and MRI features of NKTLs and DLBCLs.

Features	NKTLs	DLBCLs	*p* value
Clinical			
Age (years)	54.9 ± 15.8	59.3 ± 14.7	0.112
Gender (male/female)	46/14	16/10	0.192
Conventional MRI			
Laterality			0.627
Unilateral	37 (61.7%)	18 (69.2%)	
Bilateral	23 (38.3%)	8 (30.8%)	
Location			
Nasal cavity	54 (90.0%)	3 (11.5%)	< 0.001*
Paranasal sinus	3 (5.0%)	13 (50.0%)	< 0.001*
Frontal sinus	0 (0.0%)	0 (0.0%)	
Sphenoid sinus	0 (0.0%)	1 (3.8%)	
Ethmoid sinus	2 (4.4%)	4 (15.4%)	
Maxillary sinus	1 (2.2%)	8 (30.8%)	
Nasal cavity and paranasal sinus	3 (5.0%)	10 (38.5%)	< 0.001*
Size (mm^2)	668.7 ± 636.6	812.4 ± 536.9	0.080
Margin			0.216
Well-defined	1 (1.7%)	2 (7.7%)	
Ill-defined	59 (98.3%)	24 (92.3%)	
Signal intensity			
T1WI			0.733
Hypointense	4 (6.7%)	2 (7.7%)	
Isointense	45 (75.0%)	21 (80.8%)	
Hyperintense	11 (18.3%)	3 (11.5%)	
T2WI			0.805
Hypointense	1 (1.7%)	1(3.8%)	
Isointense	22 (36.7%)	10 (38.5%)	
Hyperintense	37 (61.7%)	15 (57.7%)	
Inner nature			0.165
Homogeneous	29 (48.3%)	17 (65.4%)	
Heterogeneous	31 (51.7%)	9 (34.6%)	
Inner component			
Cystic/necrosis	25(41.7%)	4 (15.4%)	0.025*
Hemorrhage	5 (8.3%)	3 (11.5%)	0.693
Enhancement degree			0.012*
Poor	3 (5.0%)	1 (3.8%)	
Moderate	53 (88.3%)	17 (65.4%)	
Intense	4 (6.7%)	8 (30.8%)	
Bone destruction	51 (85.0%)	24 (92.3%)	0.492
Regional invasion			
Nasal dorsum/adjacent cutaneous tissues	33 (90.0%)	13 (50.0%)	0.814
Nasopharyngeal/pterygoid region/oropharynx	29 (5.0%)	17 (65.4%)	0.165
Pterygopalatine fossa/infratemporal fossa	19 (31.7%)	19 (73.1%)	< 0.001*
Orbital cavity/pterygoid musculature	17 (28.3%)	23 (88.5%)	< 0.001*
Palate/upper alveolar process	23 (38.3%)	9 (34.6.0%)	0.573
Cervical lymph nodes	12 (20.0.8%)	7 (26.9%)	0.811
ADC value ($\times 10^{-3}$ mm^2/s)			
Polygonal ROI	0.837 ± 0.170	0.587 ± 0.090	< 0.001*
Small-round ROI	0.596 ± 0.143	0.485 ± 0.093	< 0.001*

NKTLs: natural killer (NK)/T-cell lymphomas; DLBCLs: diffuse large B-cell lymphomas; ADC: apparent diffusion coefficient; ROI: region of interest.
* p < 0.05.

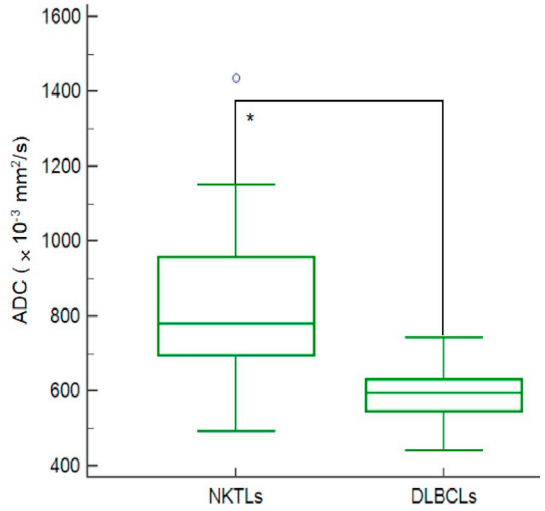

Fig. 1. Graph shows box plots of ADC value (polygonal ROI) of sinonasal NKTLs and DLBCLs. The mean ADC value is significantly higher in NKTLs than in DLBCLs (*: $p < 0.001$).

Table 2
Diagnostic performance of ADC values using different ROIs in the differentiation of NKTLs and DLBCLs.

ROI method	Cut-off ADC value	Sen (%)	Spe (%)	PPV (%)	NPV (%)	Accuracy (%)	AUC	Youden index
Polygonal	0.646[a]	80.8	90.0	77.8	91.5	87.2	0.924	0.708
Small-round	0.521[a]	69.2	71.7	51.4	84.3	70.9	0.740	0.409

Sen: sensitivity; Spe: specificity; PPV: positive predictive value; NPV: negative predictive value.
[a] $\times 10^{-3}\,mm^2/s$; AUC: area under the curve.

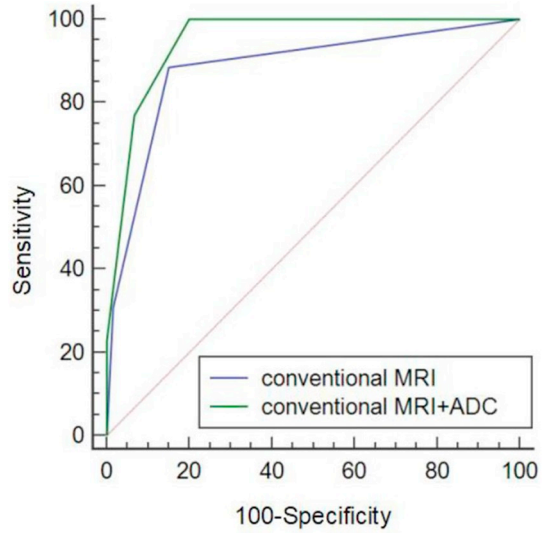

Fig. 2. ROC curves of conventional MRI and the combination of conventional MRI and ADC to differentiate between NKTLs and DLBCLs. The AUC of the combination of conventional MRI and ADC is significantly larger than that of conventional MRI, for differentiating between NKTLs and DLBCLs ($p = 0.02$).

in the nasal cavity (OR = 26.392 and 95% CI, 26.392–26.392). NKTLs were more likely to show poor (OR = 0.008 and 95% CI, 0.008–0.008) or moderate enhancement (OR = 0.025 and 95% CI, 0.025–0.025), while DLBCLs more often showed intense enhancement (OR = 0.030 and 95% CI, 0.030–0.030). Logistic regression analysis showed that the regional invasion and inner component no longer remained independent predictors for NKTLs and DLBCLs. The optimal differential performance was obtained using a cut-off ADC value of $0.646 \times 10^{-3}\,mm^2/s$ ($> 0.646 \times 10^{-3}\,mm^2/s$ for NKTLs, $\leq 0.646 \times 10^{-3}\,mm^2/s$ for DLBCLs), which generated a sensitivity of 93.3%, a specificity of 85.0% and an accuracy of 90.8% (OR = 0.975 and 95% CI, 0.956–0.994).

Three significant independent predictors were dichotomized into scores of 1 or 0 as follows: localization in the (1) nasal cavity (presence, 1; absence, 0), (2) paranasal sinus (presence, 0; absence, 1) and (3) nasal cavity and paranasal sinus (presence, 0; absence, 1); enhancement degree of (1) poor (presence, 1; absence, 0), (2) moderate (presence, 1; absence, 0) and (3) intense (presence, 0; absence, 1); and the cut-off ADC value of $0.646 \times 10^{-3}\,mm^2/s$ (> cut-off value, 1; ≤ cut-off value, 0). For each lymphoma, the sum scores were calculated from the locations and enhancement degree based on conventional MRI with various ADC values. The diagnostic performance of conventional MRI, ADC value and their combination for differentiating sinonasal NKTLs from DLBCLs is presented in Table 4 and Fig. 3, The best differential performance for conventional MRI was obtained with a cut-off score of 1, indicating that tumors located in the nasal cavity with poor or moderate enhancement were more likely to be NKTLs, with a sensitivity of 88.5%, a specificity of 85.0%, an accuracy of 86.0% and an AUC of 0.883. The best differential performance for the combination of conventional MRI and ADC value was obtained at a cut-off score of 2, indicating that tumors located in the nasal cavity with poor or moderate enhancement and ADC value $> 0.646 \times 10^{-3}\,mm^2/s$ were more likely to be NKTLs, with a sensitivity of 100.0%, a specificity of 80.0%, an accuracy of 86.0% and an AUC of 0.951. A significant difference was found between the AUC values of conventional MRI and conventional MRI in combination with ADC ($p = 0.02$) in the differentiation of NKTLs and DLBCLs.

The interreader agreement regarding the conventional MRI features ($\kappa = 0.86$) and the measurements of the ADC values (small round ROI: ICC = 0.851, CI = 0.768–0.934; polygonal ROI: ICC = 0.894, CI = 0.839–0.949) were both excellent.

Ki-67 LIs were 10% to 90% (mean 65.7 ± 18.1%) in NKTLs versus 70% to 90% (mean 83.5 ± 7.35%) in DLBCLs ($p < 0.001$). There was a poorly inverse correlation between ADC value and Ki-67 LI in the overall NHLs ($r = -0.425$, $p < 0.001$). However, there were no significant correlations between them in NKTLs or DLBCLs (both $p > 0.05$) (Table 5).

4. Discussion

In the limited studies on the imaging features of NKTLs and DLBCLs, the investigators neither made systematic differential diagnoses of the two groups of lymphomas, nor did they use advanced MRI sequences such as RESOLVE DWI [3,10,24]. For these reasons, they consistently concluded that the differentiation of tumor histologic subtypes was essentially impossible with based on imaging criteria alone [10,25]. Although CT is often used as the preferred and routine examination method for sinonasal masses, MRI offers advantages in cases of regional invasions and for tissue characterization, especially in conjunction with ADC values [26]. In present study, the location, inner nature, enhancement degree and regional invasion were demonstrated as the most valuable conventional MRI features. With the addition of ADC, an optimal sensitivity (100.0%) was achieved for the discrimination of NKTLs and DLBCLs. Our results suggested that conventional MRI combined with DWI could be applied to differentiate between sinonasal NKTLs and DLBCLs where biopsies could be hazardous.

As reported in other Asia countries [26–28], NKTLs are the most common sinonasal lymphomas in our study, 2.31 times of DLBCLs. Regarding the locations of the NKTLs and DLBCLs, studies have shown that most nasal lymphomas are NKTLs, while most paranasal lymphomas are DLBCLs and that the most commonly involved paranasal

Table 3
Logistic regression results using conventional MRI and DWI features to differentiate between NKTLs and DLBCLs.

Parameter	β Coefficient	SE	Odds ratio (95% CI)	p Value
Location 1 (sinonasal)	1.228	0.000	3.415 (3.415–3.415)	< 0.001
Location 2 (paranasal sinus)	6.433	0.000	621.771(621.771–621.771)	< 0.001
Location 3 (sinonasal & paranasal sinus)	3.273	0.000	26.392 (26.392–26.392)	< 0.001
Enhancement (poor)	−4.858	0.000	0.008 (0.008–0.008)	< 0.001
Enhancement (moderate)	−3.697	0.000	0.025 (0.025–0.025)	< 0.001
Enhancement (intense)	−3.501	0.000	0.030 (0.030–0.030)	< 0.001
ADC ($\times 10^{-3}$ mm^2/s)	−0.026	0.010	0.975 (0.956–0.994)	0.011

Note: SE: standard error; CI: confidence interval.

Table 4
Diagnostic performance of conventional MRI, ADC value and their combination for differentiating sinonasal NKTLs from DLBCLs.

Parameters	TV	Sen (%)	Spe (%)	PPV (%)	NPV (%)	Accuracy (%)	AUC
Conventional MRI	≤1	88.5	85.0	71.9	94.4	86.0	0.883
ADC	≤0.646[a]	80.8	90.0	77.8	91.5	87.2	0.924
Conventional MRI + ADC	≤2	100.0	80.0	68.4	100.0	86.0	0.951

Note. TV: threshold value.
[a] $\times 10^{-3}$ mm^2/s.

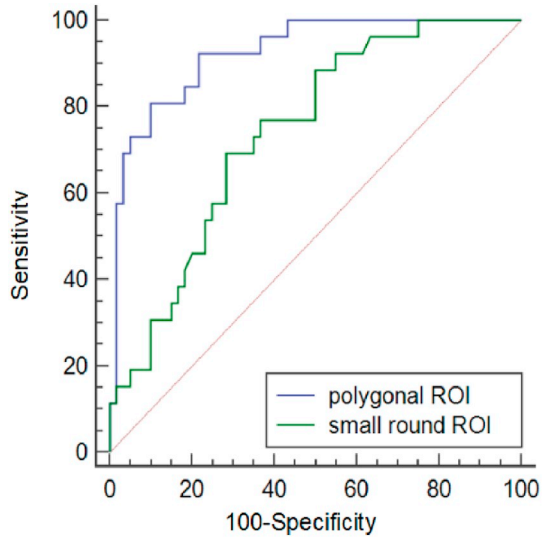

Fig. 3. ROC curves of the diagnostic efficacy of ADC values using polygonal ROI and small-round ROI to differentiate between NKTLs and DLBCLs. The AUC of polygonal ROI is significantly larger than that of small-round ROI ($p < 0.001$).

sinuses are the maxillary sinus, followed by the ethmoid sinus, sphenoid sinus and frontal sinus [24,29,30]. In agreement with the previous studies, our study suggested that the primary site of the neoplasm was the most valuable information and that it should be determined accurately when distinguishing NKTLs from DLBCLs. No previous studies have compared the enhancement degrees of NKTLs and DLBCLs in MRI. In our study, NKTLs showed less intense enhancement than did DLBCLs. This finding might be explained by the angiocentric necrosis associated with NKTLs, which means that the tumor cells infiltrate and destroy blood vessel walls [9]. Hence, although with larger extracellular space, the potentially worse microcirculation perfusion might lead to the lower enhancement degree of NKTLs.

Previous studies have suggested that bone destruction and regional invasion are important evidence supporting the stronger invasiveness of NKTLs [4,10,26,29]. However, Nakamura et al. indicated a higher bone destruction rate for DLBCLs than for NKTLs [24]. The bone destruction rates observed in our study were 84% for NKTLs and 95% for DLBCLs, indicating that NKTLs did not show stronger invasiveness than that in DLBCLs. Furthermore, the regional invasion rates by DLBCLs in locations (3) and (4) were even higher than that of NKTLs. There may be two explanations for this observation. First, logistic regression analysis indicated that it was the location of tumor and not the regional invasion that remained an independent predictor for NKTLs and DLBCLs, probably due to their close association. Second, NKTLs located in the nasal cavity that result in earlier nasal symptoms are diagnosed at an early stage, whereas DLBCLs hidden in the sinuses that induce symptoms only after extension into surrounding structures are often diagnosed at a late stage [10].

ADC values, which are derived from DWI, can quantitatively reflect the random motion of water molecules in biological tissues. However, the widely used SS-EPI approach is vulnerable to susceptibility-based distortions in the sinonasal region. The newly developed RESOLVE DWI approach significantly improves image quality, as it reduces susceptibility artifacts, distortion and blurring, which impair the conspicuity of sinonasal lesions [20]. Besides, Zhao et al. also reported that the ADC values of RESOLVE are more accurate than those of SS-EPI in the evaluation of sinonasal disease. Accordingly, the correlations between the ADC values and histopathological findings were better clarified with RESOLVE [20]. Despite some overlap in the ADC values of NKTLs and DLBCLs, we found that the mean ADC value of NKTLs was significantly higher than that of DLBCLs, which is consistent with the study of Wang et al. [1]. The histopathological basis for this difference was not well elucidated, but it could be explained by the following 3 features of NKTLs: (1) fewer tumor components and lower cellularity; (2) more necrosis and increased extracellular space; (3) lower karyoplasmic ratio [9,31]. Some meta-analyses have summarized a poorly inverse correlation between ADC and cellularity in lymphomas [16,32]. Histopathological studies indicate that NKTLs are composed of a polymorphous infiltrate in which the atypical, malignant cells are scattered among benign inflammatory cells, including eosinophils, neutrophils, histiocytes and lymphocytes. In contrast, DLBCLs are characterized by sheets of relatively monomorphic, large, diffuse infiltrates of atypical lymphocytes with little cytoplasm and cleaved or angulated nuclei [9]. Furthermore, NKTLs are characterized by angiocentricity, features related to the destruction of blood vessel walls due to tumor cell infiltration, which lead to a variable degree of localized necrosis. In contrast, B-cell lymphoma cells tend to surround and compress the blood vessels rather than invading them, resulting in limited necrosis [9].

To date, no standard ROI methods have been established for obtaining optimal ADC values [1]. In present study, the diagnostic performance of ADC values obtained using polygonal ROIs were

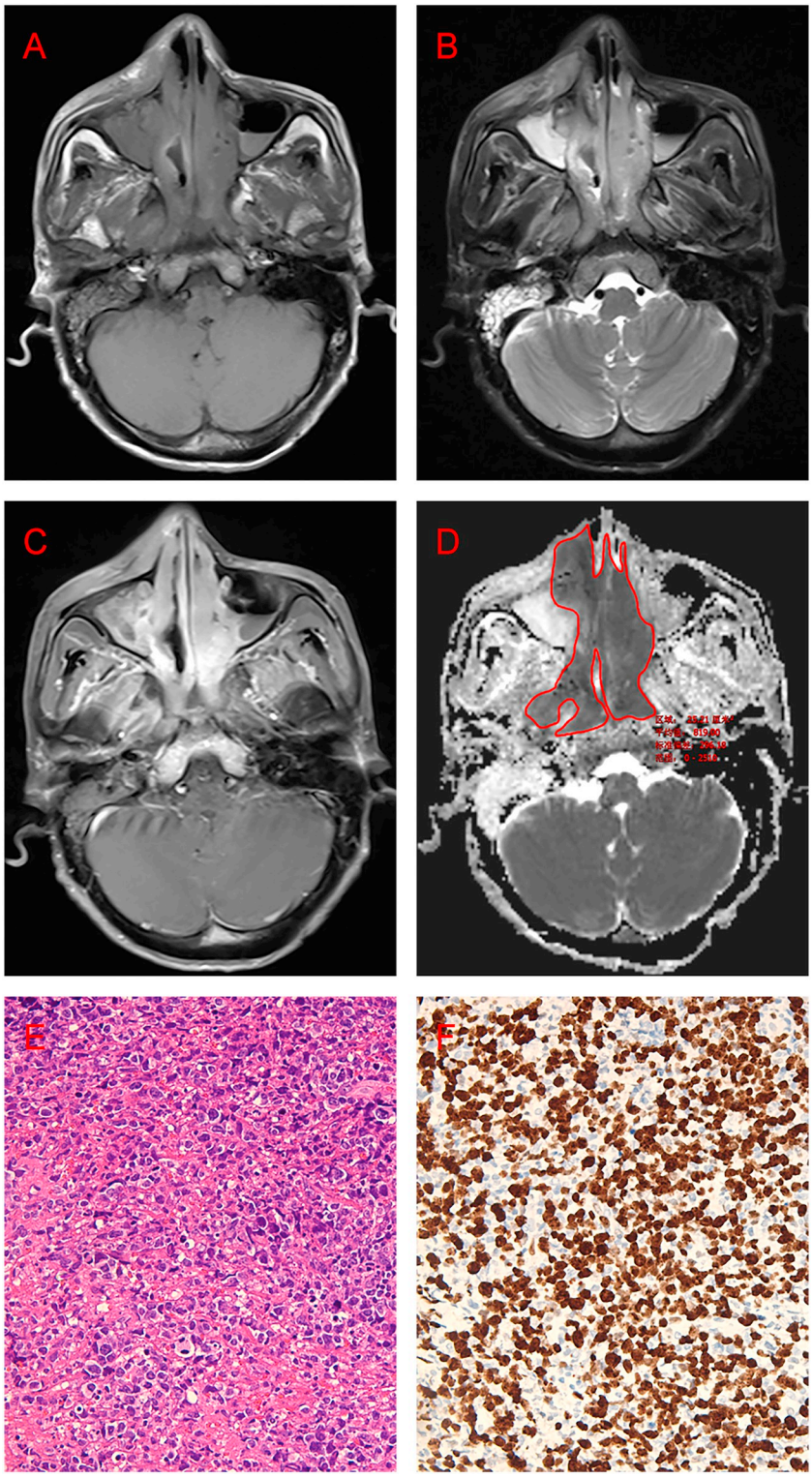

Fig. 4. A 56-year-old man with NKTL in bilateral nasal cavity and nasopharyngeal top. The tumor appears as an irregular mass with an isointense signal on axial T1-weighted image (A), a heterogeneously hyperintense signal on T2-weighted image (B) and an intensely heterogeneous enhancement (C). The tumor invades nasopharyngeal, pterygopalatine fossa, infratemporal fossa and right upper lip cutaneous tissues. (D) Axial ADC map (b = 1000 s/mm^2) shows the tumor has an ADC value of 0.819 × 10^{-3} mm^2/s using polygonal ROI. (E) Photomicrograph (H&E × 100) shows the neoplasm is composed of a mixture of polymorphous inflammatory cells and malignant atypical cells, and is characterized by angiotropism. (F) Ki-67 immunohistochemical labelling depicts that approximately 50% of cells are positive for nuclear staining.

significantly better than those obtained using small round ROIs. We propose that polygonal ROIs could better reflect the higher tumor heterogeneity of NKTLs, which might be closely related to their higher ADC values, whereas small round ROIs, which are often placed in regions with lower ADC values, were vulnerable to selection bias. Therefore, the difference in the ADC values between the two tumor types could be narrowed.

Recent studies have shown that Ki-67 expression can evaluate the proliferation and prognosis of lymphoma. However, DLBCLs with higher Ki-67 expression demonstrate a better prognosis than NKTLs. The significantly smaller mean area per Ki-67-positive cell in B-cell lymphomas and the introduction of rituximab might explain the contradictory result [33,34]. Our study manifested that Ki-67 LI of NKTLs was significantly lower than that of DLBCLs. This was in accordance with study by Yamanaka [34] et al. in the Waldeyer ring and the nasal cavity NHLs. Although Yasuda et al. [35] found no significant difference of Ki-67 expression between 11 nasal NKTLs and 16 nasal DLBCLs. Furthermore, our study showed a poorly inverse correlation between

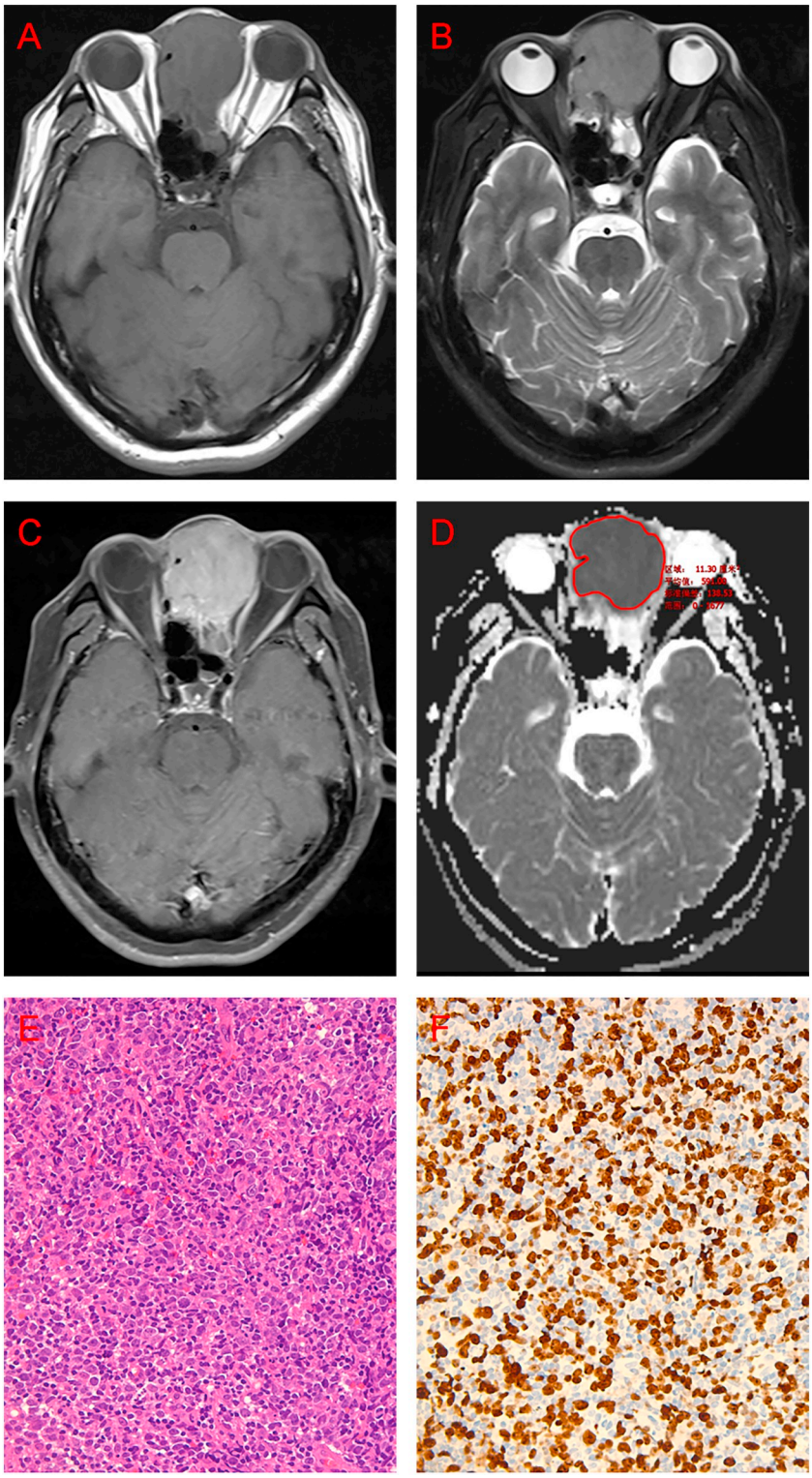

Fig. 5. A 57-year-old man with DLBCL in ethmoid sinus. The tumor appears as a homogeneous mass with an isointense signal on axial T1-weighted image (A), a slightly hyperintense signal on T2-weighted image (B) and a moderately homogeneous enhancement (C). The tumor invades orbital cavity and adjacent cutaneous tissues. (D) Axial ADC map ($b = 1000\ s/mm^2$) shows that the tumor has a low ADC value ($0.591 \times 10^{-3}\ mm^2/s$) using polygonal ROI. (E) Photomicrograph (H&E × 100) shows the neoplasm is characterized by large cells with vesicular chromatin and conspicuous nucleoli. (F) Ki-67 immunohistochemical labelling depicts that approximately 80% of cells are positive for nuclear staining (magnification, ×100).

ADC value and Ki-67 LI in the overall sample, which was consistent with studies of the central nervous system and whole body lymphomas [19, 36]. We speculated that a higher Ki-67 LI represented a higher proliferation of lymphoma cells, leading to a greater cell density, smaller extracellular space and increased karyoplasmic ratio. All these factors restricted the diffusion of water molecules and reduced ADC values [19]. Besides, no significant correlation was found between ADC value and Ki-67 LI in both subgroups. This was largely due to the mismatching between the ROI delineation and endoscopic forceps biopsy, as well as small sample size.

This study had some limitations. First, it was a single-center retrospective study with a relatively small cohort, and, therefore, selection bias was inevitable. Second, most of our patients underwent endoscopic forceps biopsy rather than surgical biopsy, and it might be not representative enough for the overall lesion of heterogeneous lymphomas.

In conclusion, our study showed that location and enhancement degree were the most valuable conventional MRI features for

Table 5
The correlation between ADC value and Ki-67 expression in subgroups of sinonasal NHLs.

Parameters	NKTLs (n = 60)	DLBCLs (n = 26)	Total (n = 86)
ADC ($\times 10^{-3}$ mm^2/s)	0.837 ± 0.170	0.587 ± 0.090	0.761 ± 0.189
Ki-67 LI (%)	65.7 ± 18.1	83.462 ± 7.317	71.047 ± 17.659
r (95% CI)	−0.071 (−0.319, 0.187)	0.003 (−0.385, 0.390)	−0.425 (−0.584, −0.234)
p value	0.591	0.989	< 0.001

NHLs: non-Hodgkin's lymphomas; NKTLs: natural killer (NK)/T-cell lymphomas; DLBCLs: diffuse large B-cell lymphomas; ADC: apparent diffusion coefficient; r: correlation coefficient; 95% CI: 95% confidence intervals; LI: labeling index.

differentiating between NKTLs and DLBCLs. The combination of MRI and RESOLVE DWI (with a cut-off ADC value of 0.646 × 10^{-3} mm^2/s) significantly improved performance in the differentiation of the two types of NHLs. ADC values may be used to noninvasively evaluate the proliferation level of sinonasal NHLs.

Grant support

This work was supported by the grant of Science and Technology Commission of Shanghai Municipality (No. 17411962100).

Declaration of Competing Interest

There is no conflict of interests.

References

[1] Wang X, Zhang Z, Chen Q, Li J, Xian J. Effectiveness of 3 T PROPELLER DUO diffusion-weighted MRI in differentiating Sinonasal lymphomas and carcinomas. Clin Radiol 2014;69(11):1149–56.
[2] Sandner A, Surov A, Bach AG, Kösling S. Primary extranodal non-Hodgkin lymphoma of the orbital and paranasal region—a retrospective study. Eur J Radiol 2013;82(2):302–8.
[3] Kim J, Kim EY, Lee S, Kim DI, Kim C, Kim S, et al. Extranodal nasal-type NK/T-cell lymphoma: computed tomography findings of head and neck involvement. Acta Radiol 2010;51(2):164–9.
[4] Hung LY, Chang PH, Lee TJ, Hsu YP, Chen YW, Fu CH, et al. Extranodal natural killer/T-cell lymphoma, nasal type: clinical and computed tomography findings in the head and neck region. Laryngoscope 2012;122(12):2632–9.
[5] Dubal PM, Dutta R, Vazquez A, Patel TD, Baredes S, Eloy JA. A comparative population-based analysis of Sinonasal diffuse large B-cell and Extranodal NK/T-cell lymphomas. Laryngoscope 2015;125(5):1077–83.
[6] Tusaliu M, Zainea V, Mogoanta CA, Dragu AA, GoanTa CM, NiTescu M, et al. Diagnostic and therapeutic aspects in malignant Sinonasal lymphoma. Rom J Morphol Embryol 2016;57(1):233–6.
[7] Chaudhary RK, Bhatt VR, Vose JM. Management of extranodal natural killer/T-cell lymphoma, nasal type. Clinical Lymphoma Myeloma and Leukemia 2015;15(5):245–52.
[8] Coiffier B, Lepage E, Briere J, Herbrecht R, Tilly H. CHOP chemotherapy plus rituximab compared with CHOP alone in elderly patients with diffuse large-B-cell lymphoma. N Engl J Med 2002;346(4):235–42.
[9] Vidal RW, Devaney K, Rinaldo A, Ferlito A, Carbone A. Clinicipathological consultation: sinonasal malignant lymphomas: a distinct clinicopathological category. Ann Otol Rhinol Laryngol 1999;108(4):411.
[10] Yen T, Wang R, Jiang R, Chen S, Wu S, Liang K. The diagnosis of sinonasal lymphoma: a challenge for rhinologists. Eur Arch Oto-Rhino-L 2012;269(5):1463–9.
[11] Xian J, Wang X, Yan F, Hao H, Wu J, Chen Q. Improved performance in differentiating benign from malignant Sinonasal tumors using diffusion-weighted combined with dynamic contrast-enhanced magnetic resonance imaging. Chinese Med J-Peking 2015;128(5):586.
[12] Tu Z, Xiao Z, Zheng Y, Huang H, Yang L, Cao D. Benign and malignant skull-involved lesions: discriminative value of conventional CT and MRI combined with diffusion-weighted MRI. Acta Radiol 2018;1286720278.
[13] Razek AAKA, Sieza S, Maha B. Assessment of nasal and paranasal sinus masses by diffusion-weighted MR imaging. J Neuroradiol 2009;36(4):206–11.
[14] Ichikawa Y, Sumi M, Sasaki M, Sumi T, Nakamura T. Efficacy of diffusion-weighted imaging for the differentiation between lymphomas and carcinomas of the nasopharynx and oropharynx: correlations of apparent diffusion coefficients and histologic features. Am J Neuroradiol 2012;33(4):761–6.
[15] Surov A, Meyer HJ, Wienke A. Associations between apparent diffusion coefficient (ADC) and KI 67 in different tumors: a meta-analysis. Part 1: ADCmean. Oncotarget 2017;8(43):75434–44.
[16] Surov A, Meyer HJ, Wienke A. Correlation between apparent diffusion coefficient (ADC) and cellularity is different in several tumors: a meta-analysis. Oncotarget 2017;8(35):59492.
[17] Schob S, Munch B, Dieckow J, Quaschling U, Hoffmann KT, Richter C, et al. Whole tumor histogram-profiling of diffusion-weighted magnetic resonance images reflects Tumorbiological features of primary central nervous system lymphoma. Transl Oncol 2018;11(2):504–10.
[18] Meyer H, Pazaitis N, Surov A. ADC histogram analysis of muscle lymphoma-correlation with histopathology in a rare entity. Br J Radiol 2018;91(1090):20180291.
[19] Sun M, Cheng J, Zhang Y, Bai J, Wang F, Meng Y, et al. Application of DWIBS in malignant lymphoma: correlation between ADC values and Ki-67 index. Eur Radiol 2018;28(4):1701–8.
[20] Zhao M, Liu Z, Sha Y, Wang S, Ye X, Pan Y, et al. Readout-segmented echo-planar imaging in the evaluation of Sinonasal lesions: a comprehensive comparison of image quality in single-shot echo-planar imaging. Magn Reson Imaging 2016;34(2):166–72.
[21] Wang F, Sha Y, Zhao M, Wan H, Zhang F, Cheng Y, et al. High-resolution diffusion-weighted imaging improves the diagnostic accuracy of dynamic contrast-enhanced sinonasal magnetic resonance imaging. J Comput Assist Tomogr 2017;41(2):199–205.
[22] Landis JR, Koch GG. The measurement of observer agreement for categorical data. Biometrics 1977;33(1).
[23] Koo TK, Li MY. A guideline of selecting and reporting Intraclass correlation coefficients for reliability research. J Chiropr Med 2016;15(2):155–63.
[24] Nakamura K, Uehara S, Omagari J, Kunitake N, Kimura M, Makino Y, et al. Primary non-Hodgkin lymphoma of the Sinonasal cavities: correlation of CT evaluation with clinical outcome. Radiology 1997;204(2):431–5.
[25] Kim JY, Lee SW, Lee JH, Suh C, Yoon DH, Lee BJ, et al. Stage IE/IIE Extranodal NK/T-cell lymphoma arising in the nasal cavity: analysis of CT findings and their prognostic value. Clin Radiol 2013;68(7):e384–90.
[26] King AD, Law BKH, Tang WK, Mo FKF, Raghupathy R, Bhatia KS, et al. MRI of diffuse large B-cell non-Hodgkin's lymphoma of the head and neck: comparison of Waldeyer'S ring and sinonasal lymphoma. Eur Arch Oto-Rhino-L 2017;274(2):1079–87.
[27] Sai A, Shimono T, Yamamoto A, Takeshita T, Ohsawa M, Wakasa K, et al. Incidence of abnormal retropharyngeal lymph nodes in sinonasal malignancies among adults. Neuroradiology 2014;56(12):1097–102.
[28] Xie C, Liu X, Mo Y, Li H, Geng Z, Zheng L, et al. Primary nasopharyngeal non-Hodgkin'S lymphoma: imaging patterns on MR imaging. Clin Imag 2013;37(3):458–64.
[29] Ou CH, Chen CC, Ling JC, Chai JW, Wu CH, Chen WH, et al. Nasal NK/T-cell lymphoma: computed tomography and magnetic resonance imaging findings. J Chin Med Assoc 2007;70(5):207–12.
[30] Wu R, Liu K, Wang W, Jin J, Song Y, Wang S, et al. Patterns of primary tumor invasion and regional lymph node spread based on magnetic resonance imaging in early-stage nasal NK/T-cell lymphoma: implications for clinical target volume definition and prognostic significance. Int J Radiat Oncol 2017;97(1):50–9.
[31] Kreisel FH. Hematolymphoid lesions of the Sinonasal tract. Head Neck Pathol 2016;10(1):109–17.
[32] Surov A, Meyer HJ, Wienke A. Correlation between minimum apparent diffusion coefficient (ADCmin) and tumor cellularity: a meta-analysis. Anticancer Res 2017;37(7):3807–10.
[33] He X, Chen Z, Fu T, Jin X, Yu T, Liang Y, et al. Ki-67 is a valuable prognostic predictor of lymphoma but its utility varies in lymphoma subtypes: evidence from a systematic meta-analysis. BMC Cancer 2014;14(1):153.
[34] Yamanaka N, Harabuchi Y, Kataura A. The prognostic value of Ki-67 antigen in non-Hodgkin lymphoma of Waldeyer ring and the nasal cavity. Cancer-Am Cancer Soc 1992;70(9):2342–9.
[35] Yasuda H, Sugimoto K, Imai H, Isobe Y, Sasaki M, Kojima Y, et al. Expression levels of apoptosis-related proteins and Ki-67 in nasal NK/T-cell lymphoma. Eur J Haematol 2009;82(1):39–45.
[36] Schob S, Meyer J, Gawlitza M, Frydrychowicz C, Müller W, Preuss M, et al. Diffusion-weighted MRI reflects proliferative activity in primary CNS lymphoma. Plos One 2016;11(8):1613–86.